

## CHAPTER 3

---

---

### PARTICLE IN CELL (PIC) SIMULATION STUDY OF STAGGER-TUNED GYRO – TWYSTRON \*

---

---

- 3.1. Introduction
- 3.2. Design of Helical Electron Beam Source (MIG)
  - 3.2.1. Single Anode (Diode) Type Magnetron Injection Gun
- 3.3. PIC Simulation Study of Stagger Tuned W-band Gyro-Twystron
  - 3.3.1. Introduction of CST Simulation Tool
  - 3.3.2. CST Modeling of Stagger Tuned W-band Gyro-Twystron
  - 3.3.3. Beam Absent or Eigen Mode Analysis
  - 3.3.4. Beam Present or Beam Wave Interaction Study
  - 3.3.5. Parametric Analysis and Validation
- 3.4. Design of Output Systems
  - 3.4.1. Design of Spent Beam Collection System or Collector
  - 3.4.2. Design of Single Disc RF Output Window
- 3.5. Conclusion

\*Part of this work has been published as:

**S. G. Yadav**, Akash and M. Thottappan, "Design and Simulation Investigations of Stagger-Tuned W-Band Gyro-Twystron," in *IEEE Transactions on Electron Devices*, vol. 69, no. 2, pp. 777-784, Feb. 2022, doi:10.1109/TED.2021.313736







### 3.1. Introduction

Since a multicavity gyro-twystron is a combination of cavities, drift tubes and waveguides, their design parameters have significant impact in the beam wave interaction mechanism and simultaneously affects the overall performance of the device.

Therefore, in the preceding chapter, Chapter 2, design of the different section, i.e., cavity, drift tube and waveguide section of the gyro-twystron amplifier have been carried out to model the amplifier device along with the detail study of bandwidth enhancement method, i.e., stagger tuning.

The present chapter emphasis on the modelling and simulation of gyro-twystron amplifier and discuss:

- In first phase each component of gyro-twystron is modelled independently with drawn design parameters. Beam absent analysis i.e. cold analysis of each section of gyro-twystron has been done to ensure the favourable the RF propagation characteristics using CST microwave studio.
- In second phase, the electron beam is introduced in study and the interaction of electron beam to RF wave is studied using PIC simulation. To optimize the performance of gyro-twystron amplifier, various parameters are varied to optimize the performance metrics.
- The design and optimization of the various sub assemblies, i.e. electron beam source, beam collector and output window, has discussed.

In the present chapter, 3D electromagnetic simulation of gyro-twystron has been done along with the modelling and simulation the various sub-assemblies of the multicavity gyro-twystron, like gyrating beam source (MIG), the interaction section, beam collector, RF window. Commercially available CST microwave studio is employed to perform

the beam absent or cold analysis of each section of gyro-twystron to ensure its frequencies (operating, resonating, and cut off) and operating modes with required quality factor. Similarly, the particle in cell (PIC) simulation is performed for the hot analysis or beam present analysis, in which the interaction of the hot electron beam and RF wave interaction is studied. The PIC simulation results predicted an output power of ~84kW at 94GHz with the gain and efficiency of ~37 dB and 22 % respectively for the beam voltage of 65kV, beam current of 6A.

In the present gyro-twystron, a single anode MIG is used to emit the gyrating electron-beam with 65 kV and 6 A with the velocity spread of 4%. Further, to collect the energy of the spent electron beams an undepressed collector is also designed along with a single disk microwave window to extract the RF output power. Also, the obtained results for the stagger tuned gyro-twystron is compared with the synchronously tuned amplifier's output, and obtained a significant enhancement in 3 dB bandwidth using stagger tuning method.

### **3.2. Design of Helical Electron Beam Source (MIG)**

The optimal performance of any gyrotron amplifier critically depends on the quality of the electron beam emitting from the electron gun or EGUN or Magnetron Injection Gun (MIG). The name MIG as it resembles a magnetron [20], forms a hollow beam of electrons in helical trajectories in the device. The name gun refers to the device's function, which is to fire a continuous stream of electrons. MIGs are available in two configurations [127],[128], diode MIGs and triode MIGs. In comparison to the triode type, which has a double anode, the diode type configuration has the simplest geometry and the more compact structure. The additional anode in the triode structure requires an additional power supply and electric insulation, making it more difficult to construct and assemble. In gyro-twystron, the effective beam-wave interaction depends

on the gyrating electron beam, and these electron beam qualities are depending on the various parameters like, pitch factor, velocity spread, beam voltage, beam current, guiding centre radius and larmor radius. The pitch factor (beam velocity ratio), a crucial parameter of electron beam, affects the device efficiency because the transverse velocity component of the gyrating beam interacts with beam waves. At high pitch factors, velocity spread increases, limiting Doppler upshifted operation, hence, limit the bandwidth. There are many factors that introduce the spread in electron velocity, such important factors are, space charge effect, roughness in the emitter surface and

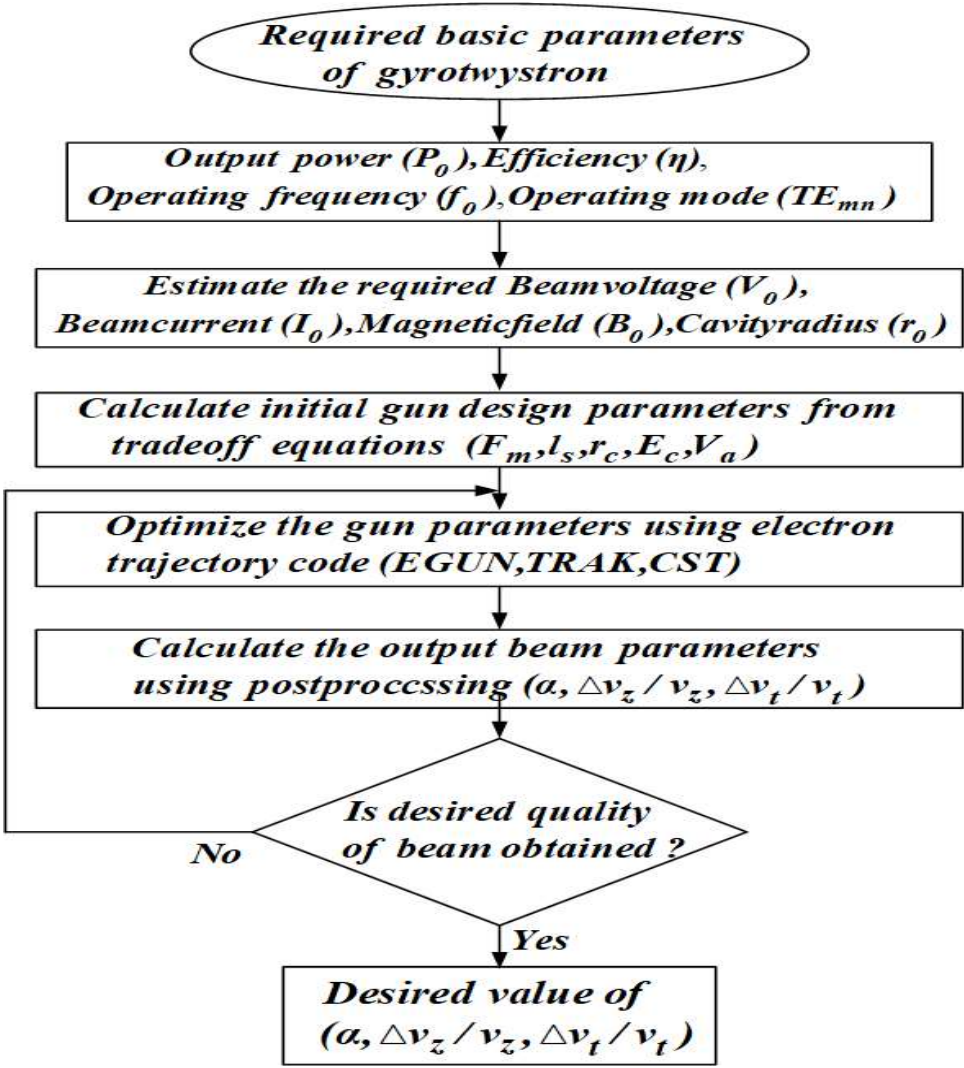


Figure 3. 1. Flow chart of design steps of a MIG.

nonuniform field near the emitter surface.

The different types of the MIG for the millimeter wave radar has been design and developed and employed in different gyro-device, like, gyro klystron, gyro-TWT and gyro-BWO, and achieved the high efficiency and wide bandwidth [129]-[132]. The design and optimization procedure of a required MIG is shown in Fig.3.1 as a flow chart.

### 3.2.1. Single Anode (Diode) Type Magnetron Injection Gun (MIG)

In the present design, a single anode (modulating and accelerating anodes are merged into a single electrode) MIG is used to emit the gyrating electron-beam with 65 kV and 6 A. The present MIG is modeled by using a 2-D electron optics' E-GUN', and the model of the gun electrode, gyrating beam profile, and magnetic field profile is shown in Figure 3.2. The design parameters of the MIG is initially depends on the required output, i.e., power, efficiency, and operating mode and calculated using the conventional trade-off equations [49],[133] and the optimized design parameters, shown in Table 3.1. The basic physical dimension of MIG, i.e., guiding center radius ( $r_g$ ), larmor radius ( $r_l$ ) and cathode radius ( $r_{cath}$ ) are interrelated, are optimized by using the equations [49],[129],[131],[133]:

$$r_g = (r_b - r_l)^{1/2} \quad [3.1]$$

$$r_l = 10^{-4} (\gamma_0 / B_0) \sqrt{(1.136 \times V_b)} \quad [3.2]$$

where,  $r_b$  is the gyrating beam radius and  $V_b$  is the beam voltage. The cathode radius is directly depends on the guiding radius and magnetic compression ratio ( $f_m$ ) as

$r_{cath} = r_g f_m^{1/2}$ . The bandwidth of the gyro amplifier is subject to the electron beam's

velocity spread; therefore, it is important to design a proper electron beam for gyro-

twystron amplifier that has optimum pitch factor and less velocity spread to ensure the best possible efficiency.

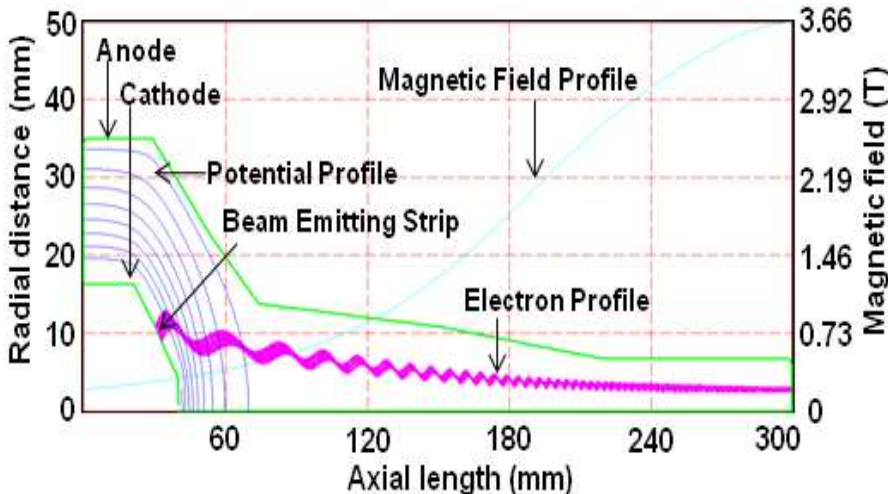


Figure 3. 2. Diode type MIG geometry, electron particle trajectory, and magnetic field profile for W-band gyro-twystron.

Table 3. 1. DESIGN PARAMETERS OF MIG FOR W-BAND GYRO-TWYSTRON [121]

Parameters	Value
Beam Voltage ( $V_b$ )	65 kV
Beam Current ( $I_b$ )	6 A
Pitch Factor ( $\alpha$ )	1.6
Velocity Spread	4%
Guiding Radius ( $r_g$ )	0.96-1.08mm
Required Magnetic Field ( $B$ )	3.66 T
Cathode Angle ( $\Phi$ )	40°
Compression ratio( $f_m$ )	28
Emitter Strip length ( $L$ )	2.5mm

The velocity spread is optimized to reduce the electron reflections, which can improve the beam quality as well as the overall performance of the device. The guiding radius is calculated as 0.9 mm, which enables the optimum beam wave interaction with the cathode loading of 8 A/cm<sup>2</sup>. The electron beam sensitivity is examined for the beams’ electrical parameters using E-GUN code. Figure 3.3 (a) and Figure 3.3 (b) show the variation of velocity ratio ( $\alpha$ ) and velocity spread for the beam current and anode voltage, respectively.

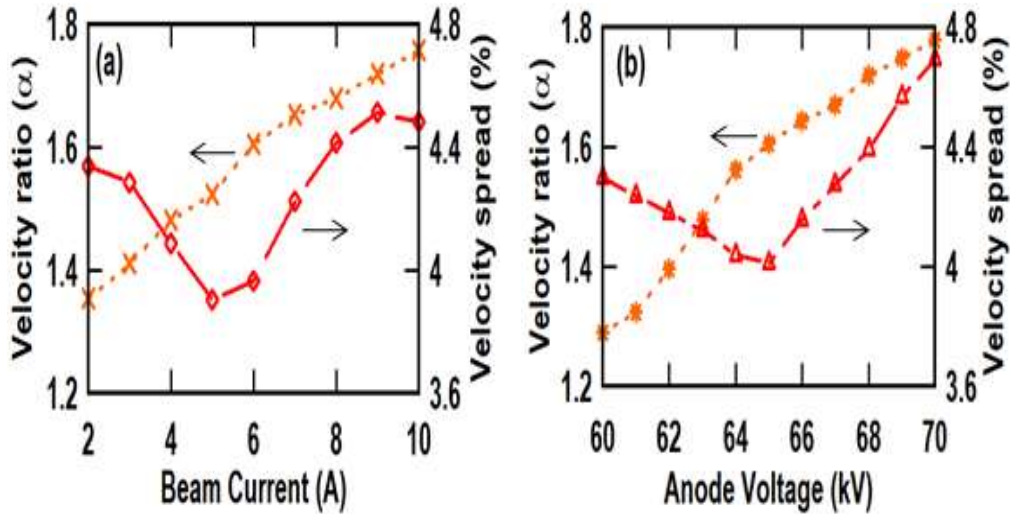


Figure 3. 3. Beam velocity ratio and velocity spread variation for different (a) beam current and (b) anode voltage

For the beam parameters of 65 kV and 6 A, the obtained the velocity ratio and velocity spread are 1.6 and 4%, respectively.

### 3.3. PIC Simulation Study of Stagger Tuned W-band Gyro-Twystron

The numerical analysis of the stager tuned gyro-twystron in Chapter 2 provides a complete representation of the device beam-wave interaction mechanism with the detail study of stagger tuning effect. However, in order to avoid manufacturing challenges, costs, and time delays, this gyro device must be virtualized in order to predict design and operation parameters. The commercially available, time-dependent, three-dimensional simulation tools allows users to virtually observe electron beam generation and beam wave interactions in the interaction region, and provide an option to optimized the design before the device is physically built.

In consideration of these advantages, it is imperative that the various simulation tolls based on different numerical techniques, such as, CST based on Finite Integration Technique (FIT), HFSS and COMSOL, based on Finite element method (FEM), XFDTD based on Finite-Difference Time-Domain method (FDTD), etc., should be included as

an integral part of design and development study of high power gyrotron devices. For the validation of the analytical finding of the present stagger tuned gyro-twystron, commercially available CST studio suit, based on finite integration technique (FIT) is used. The 3-D simulation tool gives the user a virtual environment to observe the propagation of RF waves and the gyrating beam, along with the beam wave interaction. The simulation tool can be used to investigate the operating limits of the device as well as the deleterious effect on device operation with the change in predicted parameters.

### **3.3.1. Introduction of CST PIC Simulation**

CST Particle Studio" is a fast and accurate module for analyzing the charged particle dynamics in 3D electromagnetic fields and simulating the beam wave interaction mechanism [134]. Incorporation of particles into these field calculating numerical techniques needs particle-in-cell techniques in which the particles with similar physical charge and specific mass ratio are represented as units. This macro particle representation approach incorporates the millions of unit particles to form an electron beam. Computation of Maxwell equations and Lorentz force equations are the core of PIC simulation.

CST MWS provides seven solvers for a vast range of electromagnetic problem in different structures [96]. The eigenmode solver is used to simulate closed resonant structures. The eigenmode solver is very efficient in cases of loss-free strongly resonant structures where the fields (the modes) must be calculated. With open boundaries or discrete ports, the eigenmode solver cannot be used [134]. In Eigenmode solver, either tetrahedral or hexahedral meshing is used by CST MWS. Using a hexahedral mesh, CST MWS is compatible with CST particle studio and Mphysics studio. For the cold simulation study, CST MWS is preferred over other simulation tools due to its comprehensive and flexible approach to problem-solving.

To investigate the electron beam dynamics, the particle source solver is used. In this solver an arbitrary solid surface will emit particles in accordance with a set of standard emission models. The primary responsibility of the particle tracking solver is to compute the trajectories of the particles, as well as the self-consistent electrostatic field, the space charge distribution, and the particle current.

The PIC solver, in which computation is based on of Maxwell equations and Lorentz force equations, is used to compute the RF wave and electron beam propagation as well as the beam-wave interaction. CST particle studio is based on FIT algorithm with perfect boundary approximation [96]. Unlike MAGIC-3D, CST PS PIC solver has multimode computational capabilities with additional advantages including particle tracking solver, wakefield solver.

CST Particle Studio follows four major steps before proceeding for the solution of beam-wave interaction problems. Before examining beam wave interactions with PIC simulation, a 2D cross-sectional view of the RF interaction structure must be defined for which simulation is required. The eigen mode solver is used to determine the resonating frequency and operating mode of a cavity structure in the beam absent condition or cold simulation. A waveguide port is defined at the output section of the cavity to determine the signal amplitude corresponding to the different modes. A desired cross section of an electron beam with the desired beam parameters is injected into the electromagnetic structure, using DC emission model, in order to make the beam wave interaction in interaction region. An external magnetic field must be assigned using the field solver setting to keep the electron beam focused along a predetermined path inside the interaction structure and keep in constant interaction with the RF wave. To understand the behavior of an electromagnetic device, it is necessary to have insight of the electromagnetic field distribution. Thus, required frequency points are defined at which

solver will record the fields and these field samplers are called Field Monitors. There are mainly two types of field monitor available in CST quick start guide, electric field (*E*-Field) monitor, to observe the electric field distribution and magnetic field (*H*-Field) monitor, to monitor the magnetic field distribution and these field monitors are defined in the specified dialog box. Change in particle dynamics with the time is monitored in 2D or 3D planes in terms of energy or phase, and bunching phenomena. For this, the PIC phase space monitors are defined for their momentum, energy, velocity and phase position for an interval of time. The complete process of the PIC simulation is shown in Figure 3.4, as a flow chart to illustrate the orders of PIC simulation. Before the complete design study of any device through CST PIC simulation, it has to follow some basic steps. Initially, the whole structure is modeled in CST environment, using the relevant design parameters. Second, beam absent simulation (cold simulation) or eigen mode analysis is done to choose the desired mode of operation at a desired

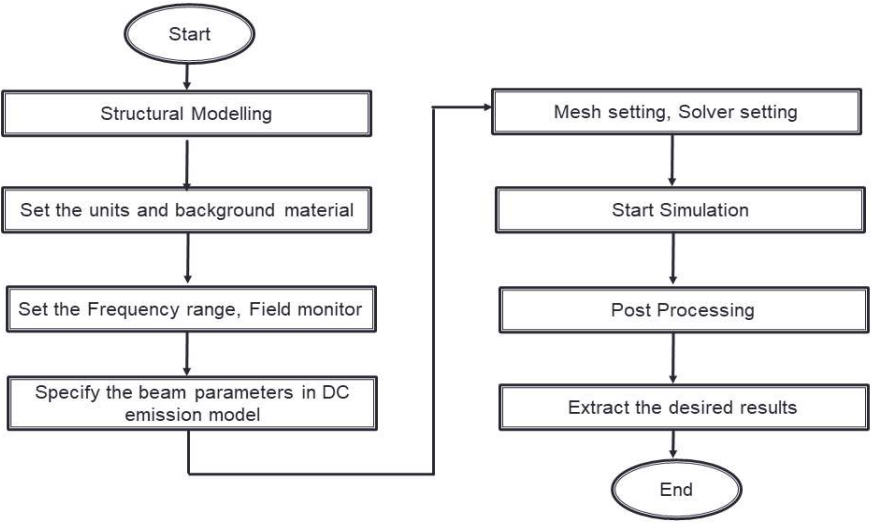
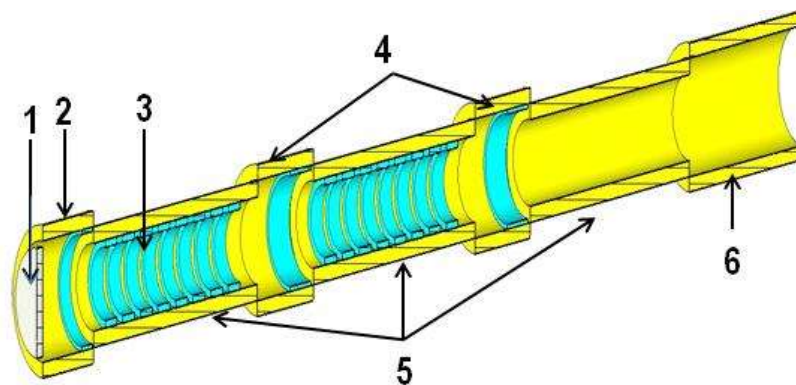


**Figure 3. 4. Flow chart illustrating the process of PIC simulation in CST environment.**

frequency. Finally, beam present simulation (hot analysis) determines the device's RF output power and gain. These processes are discussed in next section.

### 3.3.2. CST Modeling of Stagger Tuned W-band Gyro-Twystron

The present multi-cavity stagger tuned gyro-twystron [Figure 3.5] consists of three cavities and an output waveguide isolated by the drift tubes is modeled in CST environment, to observe the beam wave interaction. All cavities and the waveguide are designed to operate in a low loss azimuthally symmetric  $TE_{01}$  mode with the maximum electric field at their centre [Figure3.6]. The copper with the conductivity of  $5.8 \times 10^7$  S/m is taken as the material for the entire structure design and to reduce the ohmic losses in the structure and the background material is kept as vacuum during simulation. The complete schematic are translaed into small cells, on which Maxwell's equations and boundary conditions are solved and make the simulation fast and accurate. From the available meshing options, based on different numerical techniques, the hexahedral meshing, based on FEM, is used to translate the present desgin in to small cells. In hexhydral meshing method, first the non-manifold simulation model is created, then meshing is done on the edges and faces of the model, and finally, the complete volumes meshing, based on surface meshing, is performed [134].In mesh setting there are different parameters that controll the mesh generation and influence the design accuracy.



**1. Particle emitter 2. Input cavity 3. Dielectric rings  
4. Intermediate cavity 5. Drift Tube 6. Output waveguide**

Figure 3. 5. CST modeling of gyro-twystron.

Some important global parameters are, maximum cell and minimum cell. The maximum cell size is defined as the cell per wavelength or the highest frequency of evaluation. Similarly the minimum mesh size define the smallest permissible cell, depends on fraction of maximum cell.

The present design is meshed with 10 cells per wavelength having the smaller cell size of 0.03, the largest cell size of 0.308 and the total mesh cell of 1945633. Before starting the simulation, a perfect boundary condition is applied on the complete structure. Here the outer surface is the perfect conducting material, therefore the tangential electric field becomes zero, means boundary condition has been applied as  $E_t = 0$  at outer wall. The primary goal of using a bounding box is to reduce the complexity of solutions and also to calculate the metal loss and the dielectric loss tangent for metal surface and dielectric volume losses, respectively.

**3.3.3. Beam Absent or Eigen Mode Analysis**

The input cavity of gyro-twystron provides pre-modulated electron beam, which is modeled as its cut-off frequency is always lower than the desired operating frequency. Eigenmode analysis of the gyro-twystron cavities is carried out before the PIC using eigenmode solver to calculate resonating frequencies and operating mode (field patterns) in the absence of electron beam. The developed mode inside the cavity

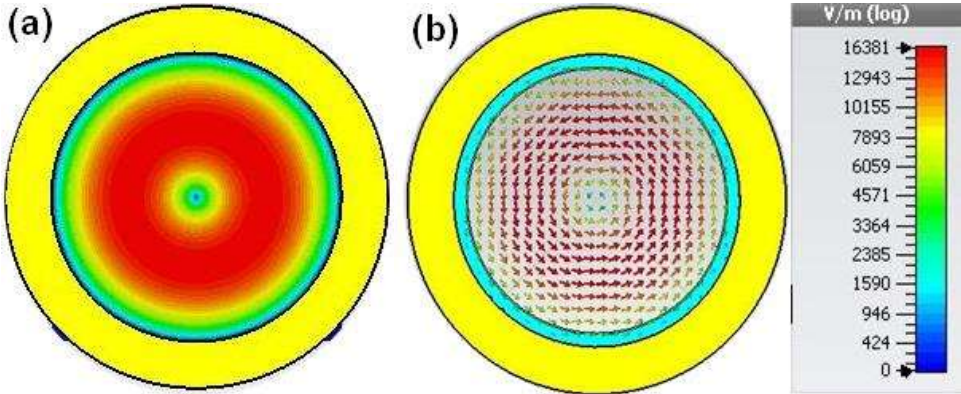


Figure 3. 6. (a) contour plot and (b) vector plot of the TE<sub>01</sub> mode in cavity.

is realized by observing the electric field pattern associated with the applied signal at the cavity's end port. The present cavities are operating in TE<sub>01</sub>, with the maximum electric field at their centre, is shown in Figure3.6. To optimize the Q-factor, the cavities is loaded with Beryllium Oxide-Silicon Carbide (BeO-SiC) dielectric rings, which is characterized by its complex dielectric constant ( $\epsilon_r = 11.52 - j3.55$ ) at 94 GHz [Figure3.7].

As the present multicavity gyro-twystron is stagger tuned, i.e., cavities are tuned at different resonating frequencies, as is confirmed in Figure3.8. 92.81 GHz, 93.73 GHz and 93.02 GHz, respectively. Ideally, these cavities are isolated from each other by the drift tube. The length ( $L_{dt}$ ) of the drift tube is fixed to provide sufficient isolation between the cavities, and its radius is calculated as small as possible using the inequality,  $r_{dt} < x_{mn}c/2\pi f$  and  $r_b < r_{dt} < r_c, r_w$ , to prevent the propagation of the operating mode. Here  $r_b$  and  $r_w$  are the gyrating beam radius and waveguide radius. The length of the drift tube section is computed using the equation 2.2, discussed in chapter 2. The drift tubes are loaded with lossy dielectric rings of BeO-SiC material to absorb any field leakage between adjacent sections and completely isolate them,

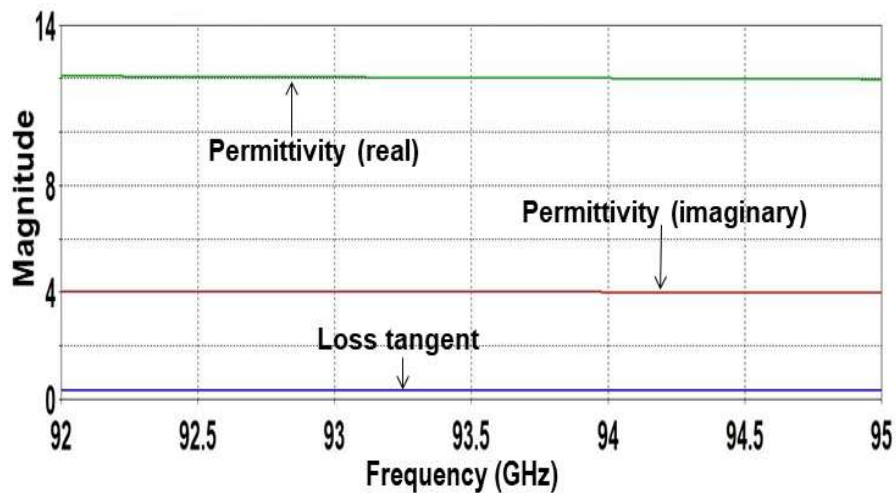


Figure 3. 7. Relative dielectric properties of BeO-SiC in W-band

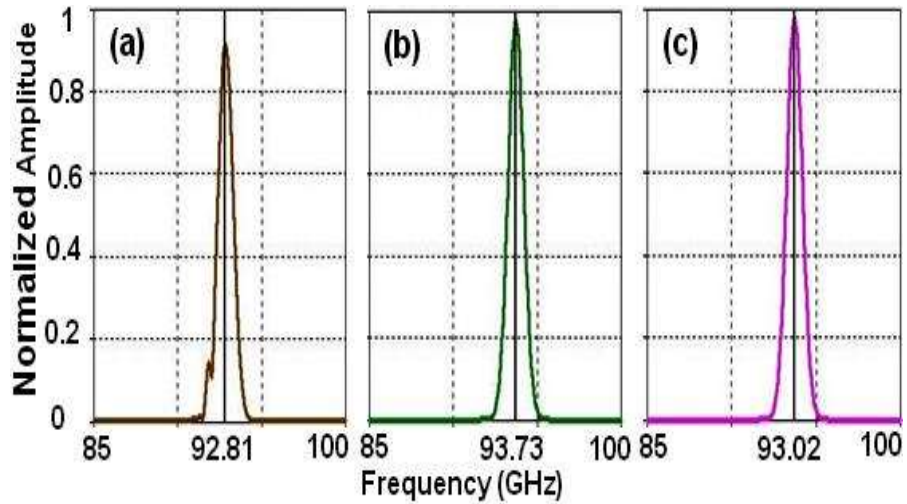


Figure 3. 8. Resonant frequency of (a) cavity I (b) cavity II and (c) cavity III.

thus suppressing spurious oscillations. In the present design, the drift tube's radius and length are calculated as  $\sim 1.45$  mm and  $\sim 14$  mm, respectively, to have the isolation of  $\sim 40$  dB between adjacent cavities and the last cavity and waveguide. The dimension of the waveguide section is decided according to the backward wave oscillation, discussed in chapter.2. The optimized design parameters are shown in Table 3.2.

Table 3. 2. DESIGN PARAMETERS FOR GYRO-TWYSTRON CIRCUIT [121]

Parameters	Cavity			Waveguide
	I	II	III	
Length (mm)	4.3	4.8	4.8	12
Radius(mm)	1.989	1.989	1.989	2.03
Operating Frequency (GHz)	92.81	93.73	93.02	94
Quality Factor	136	112	105	86

### 3.3.4. Beam Present or Beam Wave Interaction Study

The schematic of the multi cavity stagger tuned gyro-twystron is designed in beam absent condition, in CST environment. Further, for the output analysis of the present design, beam wave interaction is performed in CST particle studio. The beam wave interaction potency depends on the grating electron beam quality. The DC

emission model is used to emit the gyrating electron beams. As in the present design a single diode MIG is designed using E-GUN code, and optimized for the desired output. The optimized parameter, like, beam voltage, beam current, pitch factor, and velocity spread, as shown in Table I, are imported into the DC emission model, and developed a cathode with respect to these parameters.

To create a particle source, the shape of the emission area and the emission points are defined in DC emission model. A circular source of perfect electrical conductor (PEC) is defined as beam emitting source with many emission points. PIC simulations require grounded conducting material particle area sources. Otherwise, nonphysical charging can occur [134]. The primary cause of particle source emission in the DC Emission model is a fixed current. It can be expressed as an absolute current value (in A) or as a current density (in A/m<sup>2</sup>) [134]. To avoid high frequency problems caused by a step function, a finite rise time for the current must be defined in the current setting option of the DC emission model's particle source option [134]. After reaching that rise time, the emitting source start to emit to emit constant current/beam for the predefined time interval, as shown in Figure3.9. In DC emission model the current term is defined directly, while the voltage term is defined in term of different kinetic parameters, i.e., energy, momentum, Lorentz factor and velocity. The beam velocity ratio or pitch factor, an important parameter defining beam dynamics, is defined as inverse of tangent angle term and put in the term of angle theta in the oblique emission setting of the DC emission model. While the spread in beam velocity is directly fed as spread in kinetic setting of DC emission model. In present design 65 kV voltage is changed in velocity and the pitch factor 1.6 is changed in angle of ~58 degree. The gyrating path and the radius of the gyrating beams are defined as it avoid the collision with the structure wall, here the outer radius and inner radius is imported from the

EGUN modelling and simulation, shown in Table I and fed in emitter circle of the DC emission model. A constant DC magnetic field of  $\sim 3.66$  T is used to gyrate the electron beam along the RF interaction structure.

The emitted helical electron beams from the cathode are enter into the input cavity where it interacts with the RF input and get amplified. These amplified electrons proceed in field free drift tube and get ballistically bunched before entering to the interaction region. These pre-bunched electrons are forced into the output waveguide. The highly energetic gyrating electron beam interacts with the RF wave and transfers its kinetic energy to grow the operating  $TE_{01}$  mode. During the beam wave interaction process, some electrons gain energy while others lose energy [Figure3.10], result in a change in their relativistic mass, which in turn causes a shift in cyclotron frequency and, subsequently, a phase bunching, a significant cause of CRM interaction.

The amplified RF wave is collected at the output port in operating  $TE_{01}$  mode. The operating mode and frequency of the present stagger tuned gyro-twystron is shown [Figure 3.11], as Fast Fourier Transform (FFT) of the developed RF output signal, which confirms the mode of operation is  $TE_{01}$  mode and developed at  $\sim 94$ GHz.

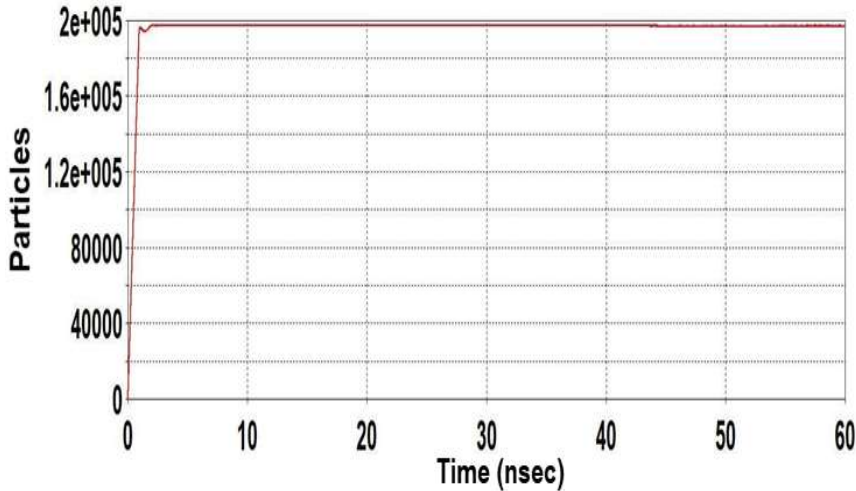


Figure 3. 9. Particle emission profile with the time interval

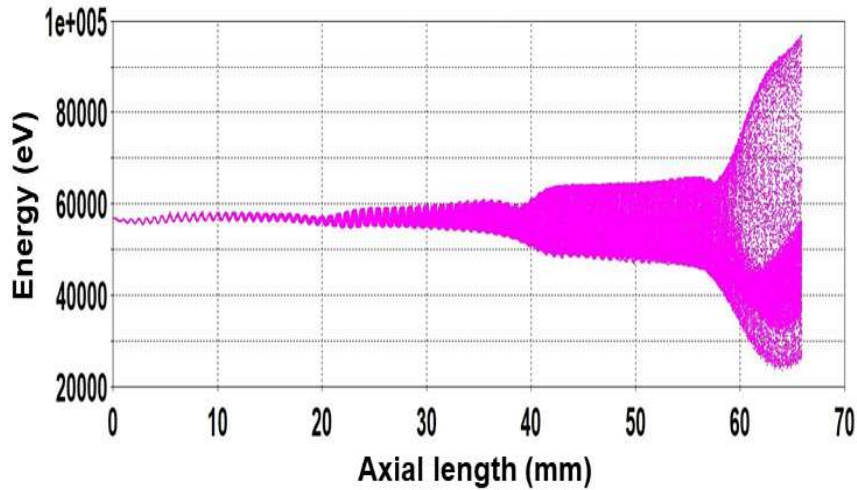


Figure 3. 10. Energy variation of electron particles with the time interval

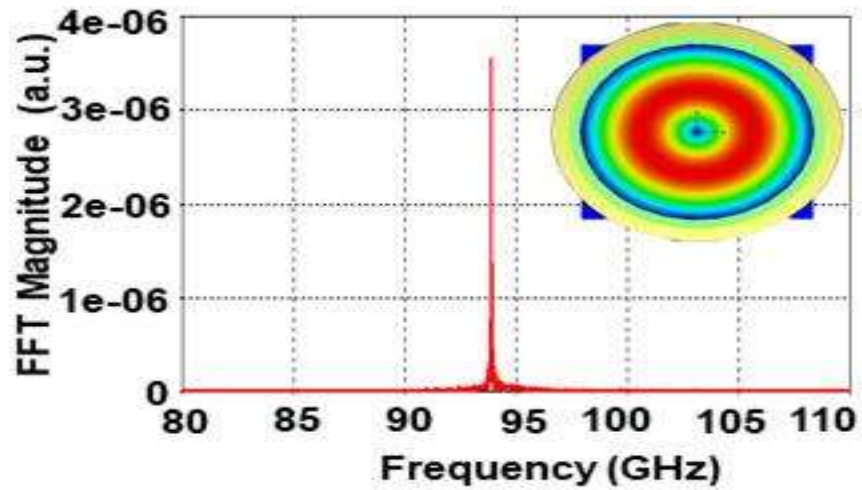


Figure 3. 11. Frequency spectrum and contour plot of the output signal at the output port.

Under the guidance of a DC magnetic field of 3.66 T, the gyrated electron beam interacts with the RF wave for a predefined time interval of 60 nsec and transmits its energy to the RF wave, and the amplified output is observed at the output port. The RF field amplitude, developed in operating  $TE_{01}$  mode at 94 GHz is shown in Figure 3.12 (a) having the maximum amplitude is  $\sim 400$  kV. The amplified amplitude used in template based post processing, and obtained the required RF output power at output port. section for the applied input RF power of 20 W. The power conversion efficiency

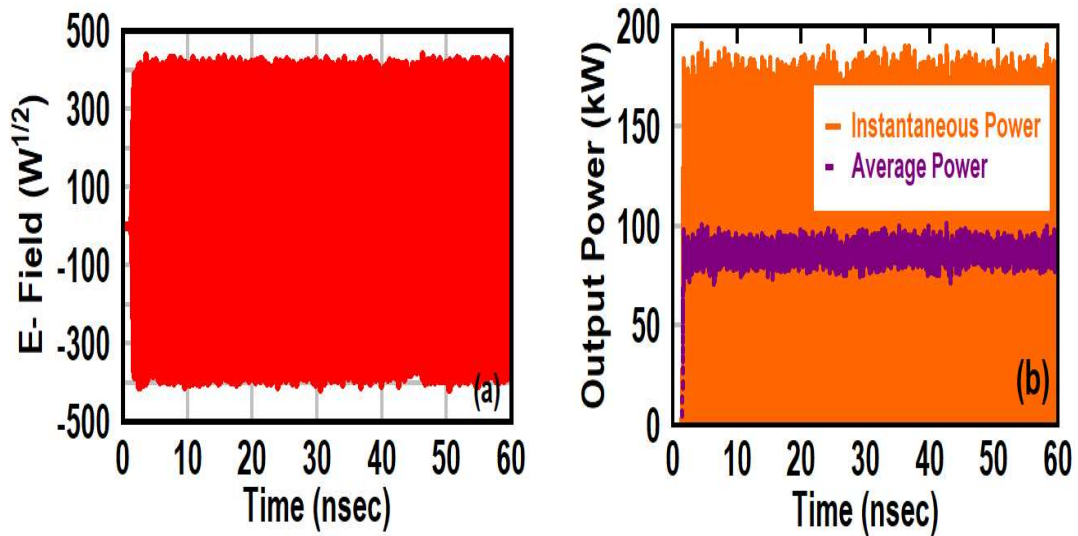


Figure 3.12. Figure 3.12 (a) Temporal growth of electric field in operating TE<sub>01</sub> mode(b) Instantaneous output power and average output power at the output port in operating TE<sub>01</sub> mode.

corresponding to the achieved RF output is ~22 % with ~36 dB gain, and full-width half maxima (FWHM) bandwidth is ~1.5 GHz.

### 3.3.5. Parametric Analysis and Validation

The parametric analysis of the gyro-twystron amplifier is carried out using the PIC simulation for the device performance evaluation in terms of gain, bandwidth, and efficiency, corresponding to the tuned parameters such as magnetic field, voltage, input

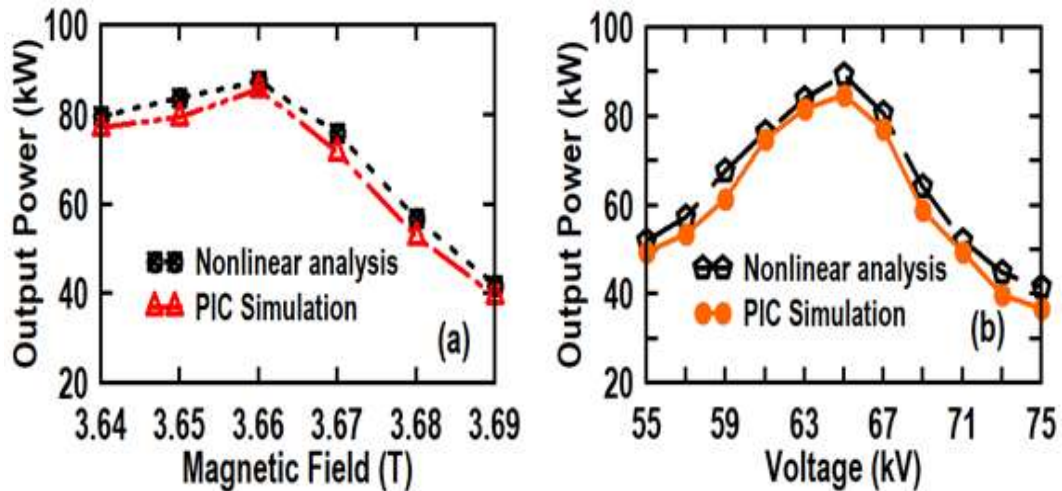


Figure 3.13. (a) RF output power as a function of magnetic field (b) RF output power as a function of applied DC voltage.

power, and velocity spread. The effect of the applied magnetic field and voltage has been investigated, as shown in Figure 3.13. Figure 3.13 (a) shows that the maximum power is achieved for the applied external DC magnetic field of 3.66 T, which provides the efficient velocity synchronization between the gyrating beam and the electromagnetic field. The applied DC voltage causes the change in relativistic factor ( $\gamma$ ) of the gyrating beam, and will change the cyclotron frequency, which affects the beam-wave interaction, thereby RF output power is varied, as shown in Figure 3.13 (b). Figure 3.14 shows the RF output power, efficiency and gain as a function of RF input

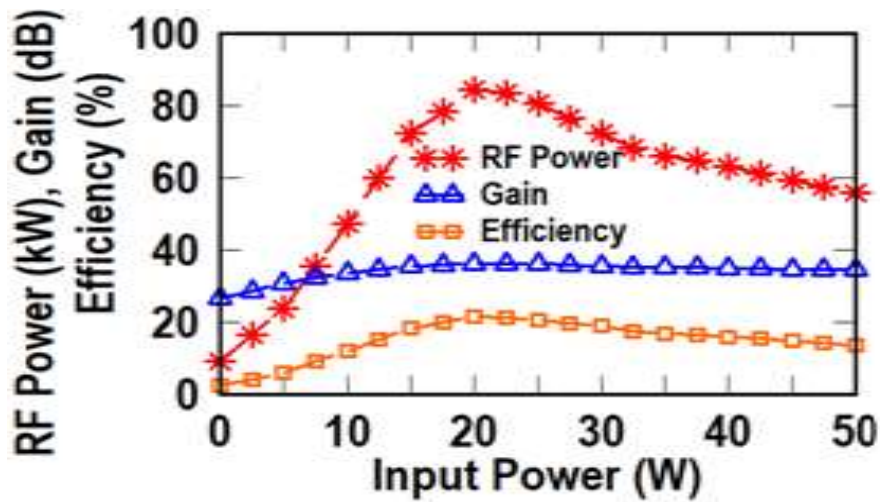


Figure 3. 14. RF power, gain and efficiency variation with the input power

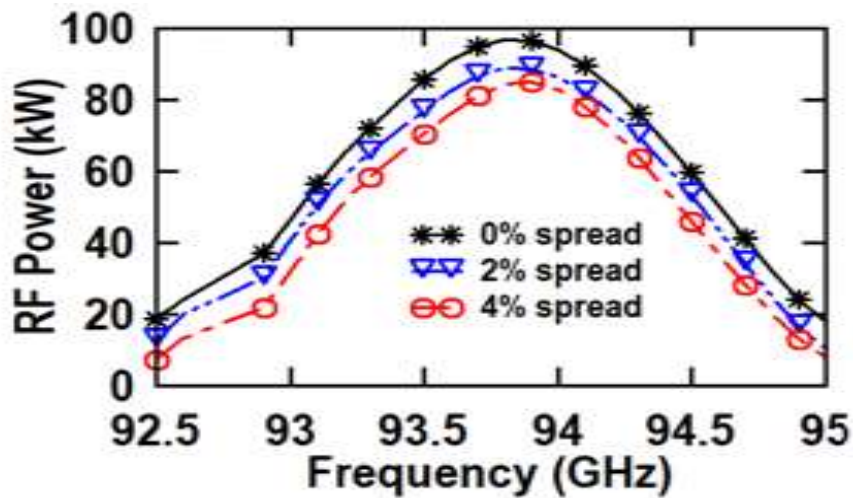


Figure 3. 15. RF output power Vs operating frequency at different velocity spread.

power corresponding to the beam voltage of 65kV and beam current of 6A at the operating frequency of 94 GHz. It is clear from the figure that the RF output power increases with the increasing input power and attain its maximum value of 83 kW at the input power of 20 W, with the gain and efficiency of ~36 dB and ~22 %, respectively. The axial beam velocity spread is an essential feature of the device, which affects the device performance by making the Doppler shift in cyclotron frequency. Figure 3.15 shows the effect of velocity spread on the output power, which influences the synchronism between the electron beam and RF wave and hence lowered the RF output power, as the spread increases. The present stagger tuned gyro-twystron , deliver 98 kW for zero velocity spread and for the velocity spread of 4 %, considered in the present design, the RF output power is 83 kW.

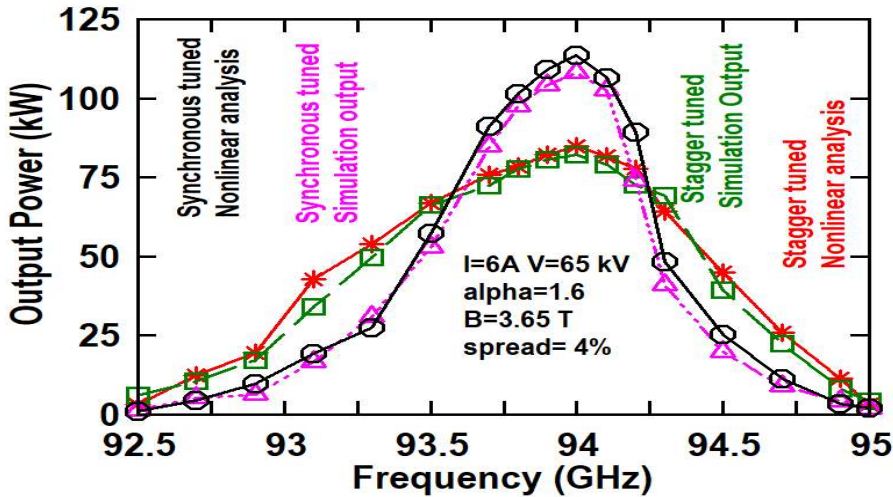


Figure 3. 16. Performance comparison of stagger tuned and synchronously tuned gyro-twystrons.

The simulation result of the present stagger tuned gyro-twystron is validated with a self-consistent nonlinear code [101] and also compared with the synchronously tuned amplifier (Figure3.16). The present study shows that the stagger-tuned gyro-twystron enhances the bandwidth ~2.5 times as compared to the synchronously tuned gyro-twystron.

### 3.4. Design of The Output System

The energised electron beam transfers its energy to the wave during beam wave interaction, but the spent electrons retain some energy. To extract the remaining energy, an undepressed collector is designed in which spent electrons are dumped and their energy is transferred as electrical energy and increases the device's overall efficiency. Design flow chart of collector is shown in Figure3.17. To extract the amplified RF output from the interaction section, a single disc RF window is required, that ensure the vacuum sealing between two different medium.

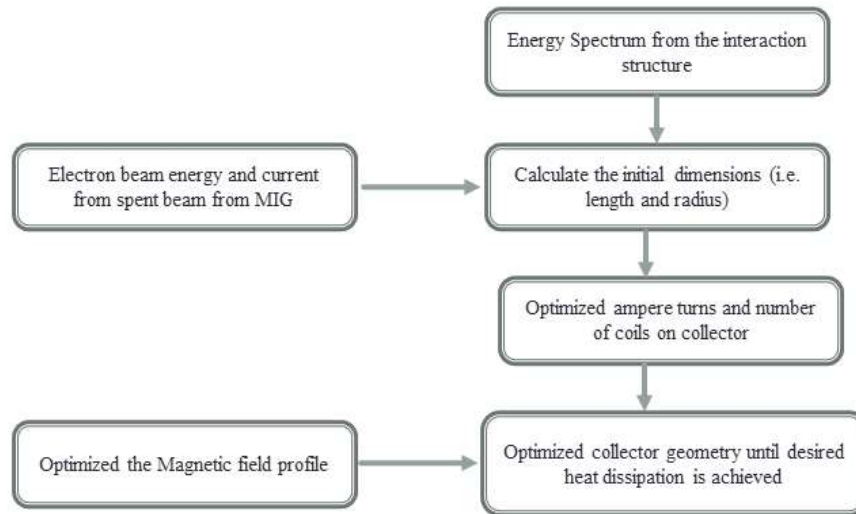


Figure 3. 17. Flow chart of collector design

#### 3.4.1. Design of Spent Beam Collection System or Collector

After the beam wave interaction, the spent electron beams still have significant energy. To recover this energy, an efficient collector is designed with proper geometry, where the kinetic energy of the electron beams converted into the electrical energy. The significant aspects considered for the collector design are maximum beam spreading, minimum heat loading on the collector wall, and maximum collector efficiency [130], [135],[136]. The trajectory of electrons inside the collector is guided by the magnetic field, which is developed by different coils. The magnetic field amplitude and

positioning of the field coil decided the beam quality inside the collector. For the beam voltage of 65 kV and current of ~6 A, the beam energy is calculated as ~390 kW and the obtained RF power after the beam wave interaction is 83 kW. The remaining 307 kW power is dissipated on the collector's inner surface. The magnetic field and the collector radius are optimized to accumulate the electron beam with an average beam power of ~30.7 kW with 10 % duty cycle. The present undepressed collector designed and optimized using the 2 D EGUN code and the electron beam trajectory and magnetic field profile in collector region is shown in Figure 3.18. The optimized length and radius of the undepressed collector are fixed as ~125 mm and ~15 mm, respectively.

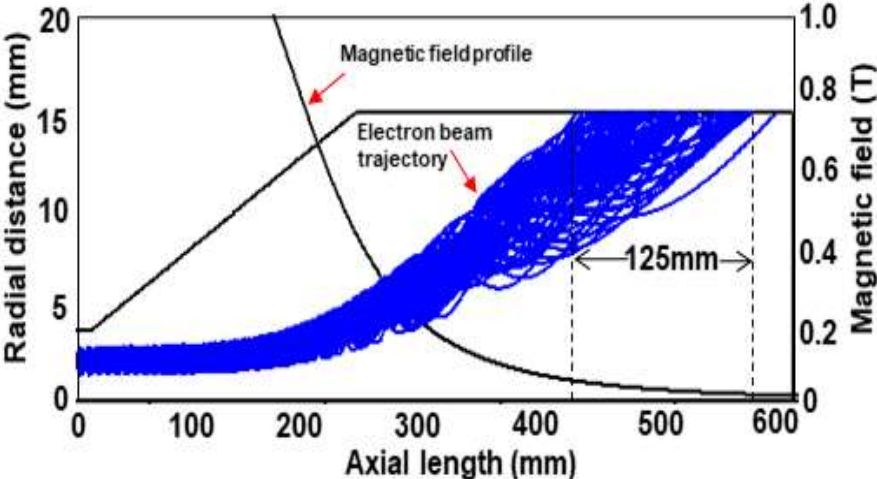


Figure 3. 18. Electron beam track and magnetic field profile in collector region.

**3.4.2. Design of Single Disc RF Output Window**

An RF window is designed to isolate the vacuum inside the device from the external environment and extract the RF output power [26],[137]. The material used for the RF window must have the minimum reflection, minimum insertion loss, high power handling capability and excellent mechanical strength. In the present single disk window design, a lossy Sapphire material is used with  $\epsilon_r = 9.4$  and  $\tan \delta = 1.5 \times 10^{-4}$ . The disc radius and thickness are calculated as ~15mm and ~0.5mm, respectively, and

optimized to provide the minimum reflection and maximum transmission at 94 GHz [Figure 3.19 (a)]. The designed window predicts less than -20 dB reflection coefficient over the ~3.2 GHz (CST simulation) and 3.1 GHz (analytical) bandwidth, respectively which is higher than the operating bandwidth (~1.5 GHz) of the gyro-twystron. It is observed that the reflection and transmission coefficients are about -50 dB and -0.1 dB, respectively [Figure 3.19 (b)], which is validated with analytical calculations [137].

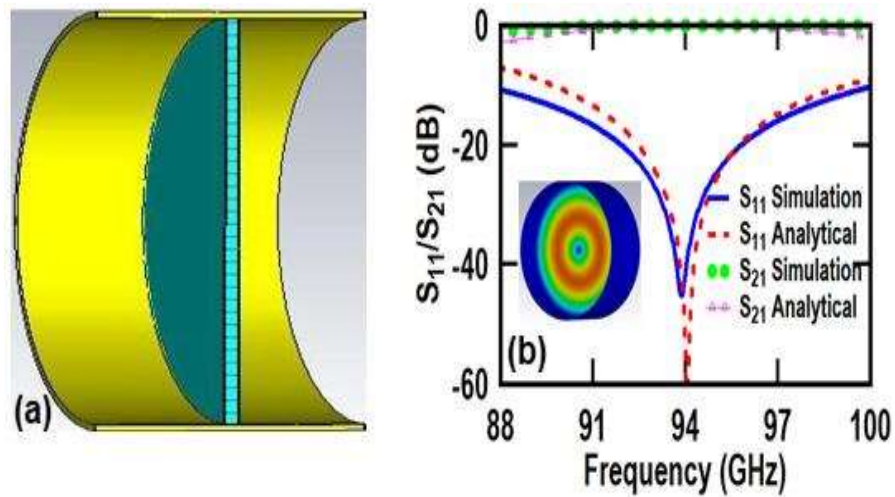


Figure 3. 19. (a) CST modeled RF window and (b) mode propagation characteristics.

### 3.5. Conclusion

In the present chapter, a multi cavity staggered tuned W-band gyro-twystron has been modeled and studied for its beam-wave interaction behavior using a commercially available 3D electromagnetic simulation tool, "CST Particle Studio". The present stagger tuned gyro-twystron has been validated with the proposed model of gyro-twystron by Blank *et al.* [121] and also validated with a nonlinear code. In the PIC simulation, cold analysis (beam absent) and hot analysis (beam present) of different sections of the stagger tuned gyro-twystron structure have been demonstrated. Cold simulation has been performed using an eigenmode solver to examine the cavity

specific mode and frequency of operation. The performance of the present stagger tuned amplifier has been improved by optimized the diode type MIG with a nominal velocity spread and compared with the synchronously tuned gyro-twystron and found that the bandwidth has been improved by ~2.5 times.

The overall finding of the present chapter is as follow:

- The PIC simulation of gyro-twystron with stagger tuned cavities has predicted an RF output power of ~84 kW with a bandwidth of 1.5 GHz. The power conversion efficiency has been calculated as ~22 % with the saturated gain of ~37 dB. The present study establishes a significant enhancement in the power-bandwidth product (126 kW-GHz) of the device, and due to this improvement, the device has the potential for being used as a high power amplifier for radar applications [121].
- In addition, a single anode MIG with 65 kV, 6 A, and 4 % spread as a particle source, a beam collector with heat loading density of 0.275 kW /cm<sup>2</sup>, and an RF output window with significant reflection and transmission characteristics have been designed and studied for the present W-band gyro-twystron.